Available online at www.sciencedirect.com
SCIENCE DIRECT
ELSEVIER
OCEAN ENGINEERING

Nonlinear free vibrations of marine risers/pipes transporting fluid

Sakdirat Kaewunruen[a], Julapot Chiravatchradej[b], Somchai Chucheepsakul[b,*]

[a]*Department of Public Works and Town and Country Planning, Ministry of Interior, Phryathai, Bangkok 10400, Thailand*
[b]*Department of Civil Engineering, King Mongkut's University of Technology, Thonburi, 91 Suksawat Road 48, Bangmod, Toongkru, Bangkok 10140, Thailand*

Abstract

An investigation emphasizing on nonlinear free vibrations of marine risers/pipes to determine the nonlinear natural frequencies and their corresponding mode shapes is presented in this paper. Based on the virtual work-energy functional of marine risers/pipes, the structural model developed consists of the strain energy due to axial deformation, strain energy due to bending, virtual works due to effective tension and external forces, and also the kinetic energy due to both the riser and the internal fluid motions. Nonlinear equations of motion coupled in axial and transverse displacements are derived through the Hamilton's principle. To analyze the nonlinear free vibrational behaviors, the system formulation has been reformed to the eigenvalue problem. The nonlinear fundamental frequencies and the corresponding numerically exact mode shapes are determined by the modified direct iteration technique incorporating with the inverse iteration. The significant influences of the marine riser's parameters studied on its nonlinear phenomena are then illustrated here first. Those parameters demonstrate the nonlinear effects due to the flexural rigidity, top tensions, internal flow velocities, and static offsets.

Keywords: Marine risers/pipes; Nonlinear free vibrations; Nonlinear frequency; Finite element; Nonlinear eigenvalue problem; Flexural rigidity; Top tension; Internal flow velocity; Static offset; Direct iteration

* Corresponding author. Tel.: +66 2470 9146; fax: +66 2427 9063.
E-mail addresses: sakdirat@hotmail.com (S. Kaewunruen), julapotc@hotmail.com (J. Chiravatchradej), somchai.chu@kmutt.ac.th (S. Chucheepsakul).

1. Introduction

Rapidly vast growth of energy industry and marine exploration signifies the incentive study of offshore structures towards utilization of floating platforms, i.e. TLPs, semisubmersibles, floating OTEC, etc. Marine riser is generally used as a fluid-conveyed curved pipe drilling crude oil, natural gas, hydrocarbon, petroleum materials, mud, and other undersea economic resources, and then transporting those to the production lines. The marine riser/pipe serves the offshore structural system as the link between the platform and the well head on the seabed. Physically, marine risers/pipes are inherently long, slender, extensible, and flexible tubular structures, and they tend to undergo the large amplitude motion subject to the severe environmental forces such as vortex shedding, current and wave forces. The marine riser traditionally consists of tugged steel pipes applied by an approximately constant top tension, and it is usually kept almost straight or nearly vertical as illustrated in Fig. 1.

The riser/pipe structure is modeled as a beam-column-like structure conveying internal fluid. The both ends are pinned supports having small static offset for which the support constraint has contributed a nonlinear axial stretching on the riser/pipe. Practically, the riser/pipe is installed along the vertical position z. After installing the drilling system, the riser/pipe encountered the current and wave forces in addition to its own weight, internal and external fluid pressures, and vessel offsets and therefore deformed to the equilibrium position. The surrounding disturbance nonlinearly perturbed the riser thus causing its vibrations. To predict more accurate vibrational behavior and trend, this investigation has been carried out for the riser statics and both linear and nonlinear free riser/pipe dynamics. The riser/pipe material considered herein is homogeneous and linear elastic obeying Hooke's law.

Various complicated aspects of marine risers/pipes transporting fluid have attracted many researchers and enlarged the number of riser/pipe investigations for over five decades. Literature reviews of the recent investigations are briefly discussed herein. Irani et al. (1987) studied the dynamic analysis of marine risers with internal steady flow and nutation dampers in three dimensions using an energy approach and the finite element method. The results indicate that the internal flow diminishes the stiffness of marine risers and it provides a negative damping mechanism. Moe and Chucheepsakul (1988) considered the effect of internal flow on vertical risers neglecting a flexural rigidity. Asymptotic approach and the finite element method were presented to obtain the linear natural frequencies. The results demonstrate that the natural frequencies are slightly reduced at a low internal flow speed but are significantly reduced at a very high flow speed. Huang (1993) derived the governing equation of kinematics of transported mass inside an extensible riser in three approaches: Lagrange, Euler, and Coriolis. Subsequently, Chucheepsakul and Huang (1994) investigated the effects of transported mass on riser equilibrium configurations with large displacements for both cases: specified top tensions and specified arc-lengths. Wu and Lou (1991) carried out a mathematical model for lateral motion of a marine riser, considering the effects of bending rigidity and internal flow. The perturbation method was applied for this investigation. It was found that the rigidity has more importance to the dynamic response of risers at high internal flow velocities. Recently, Chucheepsakul et al. (1999, 2001) studied the influence of fluid transported

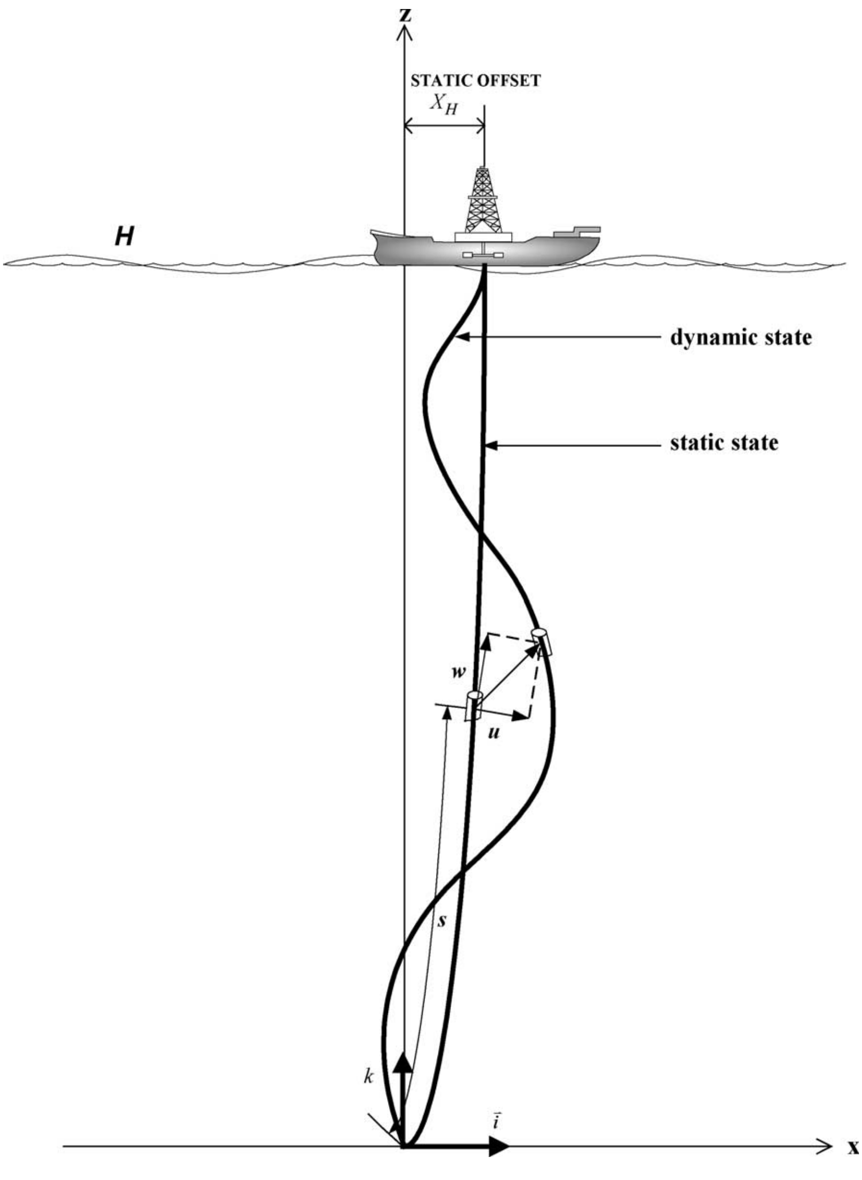

Fig. 1. Typical riser/pipe configuration.

inside the riser on its static and dynamic behaviors. The results showed that the natural frequencies of the riser decrease while both the internal flow speed and the static displacements increase; and the transported fluid reveals more significance on the high extensible risers than the low extensible ones. The effect of flexural rigidity on the static and dynamic phenomena has been investigated further through Galerkin FEM (Kaewunruen, 2003). Alternatively, the large strain formulations of marine riser have been launched to the theoretical point of view (Chucheepsakul et al., 2003). Moreover, there are numerous technical papers pertaining to the marine riser analyses (Huang and Kang, 1991; Chung et al., 1994a,b; Tikhonov et al., 1996; Atadan et al., 1997; Paidoussis, 1998; Bar-Avi, 2000; and Furnes, 2000). However, most of all investigations found in the literature review reported their results via such implicit computations for frequency domains as the finite difference, least square, perturbation technique, etc. This paper presents the nonlinear dynamic phenomena of marine riser/pipe carried out through an explicit computation in a nonlinear form of the eigenvalue problem that has never been scrutinized, nor reported previously elsewhere.

In the present study, the finite element method is applied to analyze the nonlinear free vibrations of marine riser/pipe conveying internal fluid based on the energy approach. To reach the nonlinear free vibrational behaviors, the system formulation has been reformed to the eigenvalue problem by using the Lagrange's equation of motion. The nonlinear fundamental frequencies and the corresponding numerically exact mode shapes are determined by the modified direct iteration technique incorporating with the inverse iteration. These computational algorithms are familiarized in nonlinear beam analyses (Woinowsky-Krieger, 1950; Mei, 1973; Bhashyam and Prathap, 1980; and Sarma and Varadan, 1983). The significant influences of the marine riser's parameters studied on its nonlinear vibrations are then illustrated here first. Parametric aspects demonstrate the nonlinear effects due to the modulus of elasticity, top tensions, internal flow velocities, and static offsets.

2. Variational model and formulation

The nonlinear free vibration is determined through the virtual oscillations along the marine riser. The riser will nonlinearly displace from the static equilibrium configuration due to small perturbation. Fig. 1 depicts the typical geometry of the risers in equilibrium and dynamic states. Both ends are modeled as hinged and immovable restrains. The normal displacement u and the tangential displacement w are considered to define the deformation of any point on the neutral axis of the static equilibrium configuration that was acquired from the static analysis (Huang and Chucheepsakul, 1985; Chucheepsakul and Huang, 1994).

2.1. Strain-curvature and displacement relations

Ascribed to the Euler–Bernoulli hypothesis employed in this study, the plane sections normal to centroidal axis remain plane and are normal to deformed centroidal axis. When the effect of shear deformation is considered negligible, the nonlinear strain-curvature and displacement relations can be expressed as follows

$$\kappa^* = \frac{d^2u}{ds^2} + \kappa^2 u + \frac{d\kappa}{ds} w \qquad (1)$$

$$\varepsilon = \frac{\mathrm{d}w}{\mathrm{d}s} - \kappa u + \frac{1}{2}\left(\frac{\mathrm{d}w}{\mathrm{d}s} - \kappa u\right)^2 + \frac{1}{2}\left(\frac{\mathrm{d}u}{\mathrm{d}s} + \kappa w\right)^2 \tag{2}$$

Here κ^* and κ are respected to the final and initial curvatures of the riser, for which initial one is equal to the static curvature, and ε is the axial strain due to stretching.

2.2. Element strain energy

The element strain energy of marine risers/pipes, which consists of the strain energy due to axial deformation and strain energy due to bending, is given by

$$U_\mathrm{e} = \frac{1}{2}EA\int_0^l \varepsilon^2 \mathrm{d}s + \frac{1}{2}EI\int_0^l \kappa^{*2}\mathrm{d}s \tag{3a}$$

Utilizing the Eqs. (1) and (2),

$$U_\mathrm{e} = \frac{1}{2}EA\int_0^l \left[\frac{\mathrm{d}w}{\mathrm{d}s} - \kappa u + \frac{1}{2}\left(\frac{\mathrm{d}w}{\mathrm{d}s} - \kappa u\right)^2 + \frac{1}{2}\left(\frac{\mathrm{d}u}{\mathrm{d}s} + \kappa w\right)^2\right]^2 \mathrm{d}s + \frac{1}{2}EI \times \int_0^l \left[\frac{\mathrm{d}^2u}{\mathrm{d}s^2} + \kappa^2 u + \frac{\mathrm{d}\kappa}{\mathrm{d}s}w\right]^2 \mathrm{d}s \tag{3b}$$

where E, A, I and l are the modulus of elasticity, area of the cross-section, moment of inertia of the cross-section, and element length of the riser, respectively.

2.3. Element kinetic energy

All kinetic energy terms are caused by the riser movement, and by the motion of the internal fluid flown relatively to the displacements. The element kinetic energy of marine risers/pipes consists of the kinetic energy due to riser motion and internal fluid motion as follows

$$T_\mathrm{e} = \frac{1}{2}\int_0^l m_\mathrm{r}\left[\dot{u}^2 + \dot{w}^2\right]\mathrm{d}s + \frac{1}{2}\int_0^l m_\mathrm{f}\left[(\dot{u} + Vu')^2 + (\dot{w} + Vw')^2\right]\mathrm{d}s \tag{4}$$

where T_e is the element kinetic energy, m_r is the riser mass per length, m_f is the internal fluid mass per length, and $(\cdot)$ represents the derivative respect to time t.

2.4. Virtual work done due to external forces

Needed for static and dynamic response analyses, $\delta\Omega_\mathrm{e} = \delta W_\mathrm{e} + \delta W_\mathrm{F} + \delta W_\mathrm{I}$, the virtual work done due to external forces such as the effective weight, hydrodynamic forces, and inertia forces are taken into account for accurate reckons. On the unification of the actual riser weight W, internal and external fluid pressures, and the oceanic buoyancy, the effective weight w_e, $w_\mathrm{e} = W + \gamma_\mathrm{i}A_\mathrm{i} - \gamma_0 A_0$, institutes the virtual work done δW_e given by

$$\delta W_{\mathrm{e}} = -\int_0^l w_{\mathrm{e}} \delta w \, \mathrm{d}s \tag{5}$$

Following is the virtual work done due to hydrodynamic forces that are decomposed into two directions of the current velocities: one in normal direction F_{n} associated with normal current velocity V_{n}, and another in tangential direction F_{t} associated with tangential current velocity V_{t}.

$$\delta W_{\mathrm{F}} = -\int_0^l [F_{\mathrm{n}} \delta u + F_{\mathrm{t}} \delta w] \mathrm{d}s \tag{6}$$

where

$$F_{\mathrm{n}} = \frac{1}{2} \rho_{\mathrm{w}} D_{\mathrm{O}} C_{\mathrm{Dn}} (V_{\mathrm{n}} - \dot{u}) |V_{\mathrm{n}} - \dot{u}| + \rho_{\mathrm{w}} A_{\mathrm{OH}} C_{\mathrm{M}} \dot{V}_{\mathrm{n}} - \rho_{\mathrm{w}} A_{\mathrm{OH}} C_M - 1 \ddot{u} \tag{7}$$

$$F_{\mathrm{t}} = \frac{1}{2} \rho_{\mathrm{w}} D_{\mathrm{O}} C_{\mathrm{Dt}} (V_{\mathrm{t}} - \dot{w}) |V_{\mathrm{t}} - \dot{w}| + \rho_{\mathrm{w}} A_{\mathrm{OH}} C_{\mathrm{M}} \dot{V}_{\mathrm{t}} - \rho_{\mathrm{w}} A_{\mathrm{OH}} C_M - 1 \ddot{w} \tag{8}$$

Here, sea density is denoted by ρ_w, hydrodynamic cross-sectional area by A_{OH}, inertia coefficient by C_M, normal drag force coefficient by C_{Dn}, tangential drag force coefficient by C_{Dt}, and outer diameter by D_O.

Occurring when there is a virtual oscillation of the riser and it then perturbs the surrounding water—inducing inertia forces, the virtual work done due to inertia forces δW_{I} is expressed as follows

$$\delta W_{\mathrm{I}} = -\int_0^l [(m_{\mathrm{r}} a_{\mathrm{ru}} + m_{\mathrm{f}} a_{\mathrm{fu}}) \delta u + (m_{\mathrm{r}} a_{\mathrm{rw}} + m_{\mathrm{f}} a_{\mathrm{fw}}) \delta w] \mathrm{d}s \tag{9}$$

note that,

$$a_{\mathrm{ru}} = \ddot{u} \tag{10a}$$

$$a_{\mathrm{rw}} = \ddot{w} \tag{10b}$$

$$a_{\mathrm{fu}} = \left(\frac{\partial}{\partial t} + V \frac{\partial}{\partial s} \right)^2 u = \ddot{u} + 2V\dot{u}' + \dot{V}u' + V^2 u'' \tag{11}$$

$$a_{\mathrm{fw}} = \left(\frac{\partial}{\partial t} + V \frac{\partial}{\partial s} \right)^2 w = \ddot{w} + 2V\dot{w}' + \dot{V}w' + V^2 w'' \tag{12}$$

In Eqs. (11) and (12), V represents the internal flow speed and $\dot{V}$ is the internal flow acceleration.

3. Finite element model

Referring to Fig. 1, the nodal displacements of the 4 degree-of-freedom (dof) element could be found by applying the cubic polynomial displacement function as the displacement fields to the configuration approximation. These displacement fields are given in terms of the arc-length (s) and cubic polynomial coefficients (a_i) by

$$u = a_1 + a_2 s + a_3 s^2 + a_4 s^3 \tag{13}$$

$$w = a_5 + a_6 s + a_7 s^2 + a_8 s^3 \tag{14}$$

Consequently with some mathematical manipulations, the displacement vector $\{u\}$ can be expressed in the matrix relationships between the nodal degree of freedom of the element $\{d\}$ and shape functions $[N]$ as follows.

$$\{u\} = \begin{Bmatrix} u \\ w \end{Bmatrix} \cong [N]\{d\} \tag{15}$$

The shape function matrix $[N]$ described above is

$$[N] = \begin{bmatrix} N_1 & N_2 & 0 & 0 & N_3 & N_4 & 0 & 0 \\ 0 & 0 & N_1 & N_2 & 0 & 0 & N_3 & N_4 \end{bmatrix} \tag{16}$$

where N_1, N_2, N_3, and N_4 are the cubic shape functions for the beam element (Cook et al., 1998).

The nodal degree of freedom of the riser element $\{d\}$ consists of

$$\{d\} = \lfloor u_1 \quad u_1' \quad w_1 \quad w_1' \quad u_2 \quad u_2' \quad w_2 \quad w_2' \rfloor^T \tag{17}$$

3.1. Linear and nonlinear stiffness matrices

At the state of motions, to achieve both linear and nonlinear stiffness matrices, the nonlinear strain-curvature displacement relations defined in Eqs. (2) and (3) are governed into the matrix formulation. From the relationships between the displacement vector and the nodal displacement vector in Eq. (15), the change of curvature κ^* and the nonlinear axial strain ε_d could be invented in matrix forms below

$$\kappa^* = \lfloor A \rfloor [G]\{d\} \tag{18}$$

$$\varepsilon = \varepsilon_0 + \lfloor P \rfloor [G]\{d\} + \frac{1}{2}\{d\}^T[G]^T[H][G]\{d\} \tag{19}$$

where, ε_0 stands for static strain, and

$$\lfloor A \rfloor = \lfloor \kappa^2 \quad 0 \quad 1 \quad \kappa' \quad 0 \rfloor \tag{20}$$

$$[G] = \begin{bmatrix} N_1 & N_2 & 0 & 0 & N_3 & N_4 & 0 & 0 \\ N_1' & N_2' & 0 & 0 & N_3' & N_4' & 0 & 0 \\ N_1'' & N_2'' & 0 & 0 & N_3'' & N_4'' & 0 & 0 \\ 0 & 0 & N_1 & N_2 & 0 & 0 & N_3 & N_4 \\ 0 & 0 & N_1' & N_2' & 0 & 0 & N_3' & N_4' \end{bmatrix} \tag{21}$$

$$[H] = \begin{bmatrix} \kappa^2 & 0 & 0 & 0 & -\kappa \\ 0 & 1 & 0 & \kappa & 0 \\ 0 & 0 & 0 & 0 & 0 \\ 0 & \kappa & 0 & \kappa^2 & 0 \\ -\kappa & 0 & 0 & 0 & 1 \end{bmatrix} \tag{22}$$

$$\lfloor P \rfloor = \lfloor -\kappa \quad 0 \quad 0 \quad 0 \quad 1 \rfloor \tag{23}$$

By substituting Eqs. (18) and (19) into Eq. (3), the element strain energy is rewritten as,

$$U_e = \frac{1}{2}\{d\}^T \left([k] + \frac{1}{3}[n_1] + \frac{1}{6}[n_2] \right)\{d\} \tag{24}$$

Pertaining to Eq. (24), the linear element stiffness matrix $[k]$, the first-order-nonlinear incremental stiffness matrix $[n_1]$, and the second-order-nonlinear counterpart $[n_2]$ are presented, respectively, by

$$[k] = \int_0^l (T_Z[G]^T[H][G] + EA[G]^T \lfloor P \rfloor^T \lfloor P \rfloor [G])\mathrm{d}s + EI \times \int_0^l [G]^T \lfloor A \rfloor^T \lfloor A \rfloor [G]\mathrm{d}s \tag{25}$$

$$[n_1] = \frac{3}{2}EA \int_0^l [G]^T \lfloor P \rfloor^T \{d\}^T [G]^T [H][G]\mathrm{d}s + \frac{3}{2}EA \int_0^l [G]^T[H][G] \times \{d\} \lfloor P \rfloor [G]\mathrm{d}s \tag{26}$$

$$[n_2] = \frac{3}{2}EA \int_0^l [G]^T[H]^T[G]\{d\}\{d\}^T[G]^T[H][G]\mathrm{d}s \tag{27}$$

Note that T_Z represents the nodal static top tension, which is computed from the static strain ε_0.

3.2. Mass matrix

Reckoned from two parts: riser and internal fluid, the mass matrix comprises of the riser mass matrix and the internal fluid density matrix. The replacement of Eq. (15) in Eq. (4)

yields

$$T_{\mathrm{e}} = \frac{1}{2}\{\dot{d}\}^{\mathrm{T}}[\hat{m}_{\mathrm{r}}]\{\dot{d}\} + \frac{1}{2}\{\dot{d}\}^{\mathrm{T}}[\hat{m}_{\mathrm{f}}]\{\dot{d}\} + \frac{1}{2}\{\dot{d}\}^{\mathrm{T}}[\underset{\dots}{m}_{\mathrm{f}}]\{d\} + \frac{1}{2}\{d\}^{\mathrm{T}}[\underset{\sim}{m}_{\mathrm{f}}]\{d\} \tag{28}$$

in which, the vector of nodal velocity $\{\dot{d}\}$ is

$$\{\dot{d}\} = \lfloor \dot{u}_1 \quad \dot{u}'_1 \quad \dot{w}_1 \quad \dot{w}'_1 \quad \dot{u}_2 \quad \dot{u}'_2 \quad \dot{w}_2 \quad \dot{w}'_2 \rfloor^T \tag{29}$$

and the matrices of riser mass $[\hat{m}_r]$ and internal fluid density $[\hat{m}_f]$, the gyroscopic matrix $[\underset{\dots}{m}_f]$, and the centrifugal matrix $[\underset{\sim}{m}_f]$, are given consecutively by

$$[\hat{m}_{\mathrm{r}}] = m_{\mathrm{r}} \int_0^l [N]^{\mathrm{T}}[N]\mathrm{d}s \tag{30}$$

$$[\hat{m}_{\mathrm{f}}] = m_{\mathrm{f}} \int_0^l [G]^{\mathrm{T}}[W]^{\mathrm{T}}[W][G]\mathrm{d}s \tag{31}$$

$$[\underset{\dots}{m}_{\mathrm{f}}] = 2m_{\mathrm{f}}V \int_0^l [G']^{\mathrm{T}}[W]^{\mathrm{T}}[W][G]\mathrm{d}s \tag{32}$$

$$[\underset{\sim}{m}_{\mathrm{f}}] = m_{\mathrm{f}}V^2 \int_0^l [G]^{\mathrm{T}} \lfloor A \rfloor^{\mathrm{T}} \lfloor A \rfloor [G]\mathrm{d}s \tag{33}$$

where

$$[W] = \begin{bmatrix} 1 & 0 & 0 & 0 & 0 \\ 0 & 0 & 0 & 1 & 0 \end{bmatrix} \tag{34}$$

3.3. Equation of motion in matrix form

To investigate the nonlinear free vibrations of marine risers/pipes, the global assembled Eqs (24) and (28) have been applied to Lagrange's equation, reforming the system formulations to eigenvalue problem as a nonlinear global governing matrix. With respect to D_i, the vector of the riser's global degree of freedom, the Lagrange's equation is put by

$$\frac{\mathrm{d}}{\mathrm{d}t}\frac{\partial(T-U)}{\partial\dot{D}_i} - \frac{\partial(T-U)}{\partial D_i} \tag{35}$$

After substituting the global assembled Eqs. (24) and (28) in Lagrange's Eq. (35), the equation of motion is expressed as

$$[M]\{\ddot{D}\} + [G_r]\{\dot{D}\} + \left([K] + \frac{1}{2}[N_1] + \frac{1}{3}[N_2]\right)\{D\} = \{0\} \tag{36}$$

while each of global matrices is

$$[M] = \sum_{i=1}^{\mathrm{Nel}}[\hat{m}_{\mathrm{r}}]_i + \sum_{i=1}^{\mathrm{Nel}}[\hat{m}_{\mathrm{f}}]_i \tag{37}$$

$$[G_{\mathrm{r}}] = \sum_{i=1}^{\mathrm{Nel}} [\underset{\dots}{m}_{\mathrm{f}}]_i \tag{38}$$

$$[K] = \sum_{i=1}^{\mathrm{Nel}} [k]_i - \sum_{i=1}^{\mathrm{Nel}} [\underset{\sim}{m}_{\mathrm{f}}]_i \tag{39}$$

$$[N_1] = \sum_{i=1}^{\mathrm{Nel}} [n_1]_i \tag{40}$$

$$[N_2] = \sum_{i=1}^{\mathrm{Nel}} [n_2]_i \tag{41}$$

3.4. Linear free vibrations of marine risers/pipes

Linear frequencies and the corresponding mode shapes found are obviously in very good agreement with the previous tasks (Chucheepsakul et al., 1999). Schematically, by depriving the nonlinear terms—$[N_1]$ and $[N_2]$ in Eq. (36)—remains the same linear matrix equation. The orderly matrix equation is imposed by the particular boundary conditions. Then, to reap the linear FEM solutions, the generic finite element method (FEM) is applied to the recent matrix equation of motion.

Analytically extracted throughout the Eq. (36), the linearized problem has the harmonic solution for complex eigenvalue $\lambda_i = a_i + i\omega_i$ in the form

$$\{D\} = \{\tilde{D}\}\mathrm{e}^{\lambda t} \tag{42}$$

in which ω_i is the natural frequency and $\{\tilde{D}\}$ is the corresponding mode shape. Replacing Eq. (42) into the linearized equation yields the second order eigenvalue problem

$$\{\lambda^2[M] + \lambda[G] + [K]\}\{\tilde{D}\} = \{0\} \tag{43}$$

The generalized eigenvalue problem can be obtained by transforming Eq. (42) into the following form

$$[H]\{Z\} = \lambda\{Z\} \tag{44}$$

where

$$[H] = \begin{bmatrix} -[M]^{-1}[G] & -[M]^{-1}[K] \\ [I] & 0 \end{bmatrix} \tag{45}$$

$$\{Z\} = \begin{Bmatrix} \dot{\tilde{D}} \\ \tilde{D} \end{Bmatrix} \tag{46}$$

The matrix $[H]$ is real, nonsymmetrical matrix. The eigenvalue problem, in Eq. (44), is eventually solved by QZ algorithm.

3.5. Nonlinear dynamics of marine risers/pipes

Noting that the point of maximum amplitude is of interest and recalling the singular, nonlinear equations of motion, the Eq. (36) can be maneuvered to the specific equation system by defining the time-dependent function at the reversal point of global motion at all instances of time as

$$\{\ddot{D}\}_{\max} = -\omega_{\mathrm{N}}^2\{D\}_{\max} \tag{47a}$$

$$\{\dot{D}\}_{\max} = \{0\} \tag{47b}$$

in which ω_{N} represents the nonlinear natural frequency of the riser. Throughout the nonlinear computation, the deflected shape basically does not vary with time and the time variation of the displacements is fundamentally assumed as the harmonic function, thereby the Eq. (44) simply yields the so-called nontrivial solution.

Consequently, at the time to maximum velocity, the particular, governing, nonlinear eigenproblem matrix is accomplished by superceding Eqs. (47a,b) into (36), for which

$$\left([K] + \frac{1}{2}[N_1] + \frac{1}{3}[N_2] - \omega_{\mathrm{N}}^2[M]\right)\{D\}_{\max} = \{0\} \tag{48}$$

For numerically exact solutions at maximum amplitude, the familiar modified direct iteration technique incorporating with the inverse iteration are applied to solve the system of nonlinear equations (Eq. (48)) through the following procedure. As aforementioned, the linear frequencies are first obtained by QZ algorithm and the corresponding linear mode shapes are normalized with the maximum amplitude sought. The reference amplitude is enumerated at the point having maximum displacements searched throughout its mode. The nonlinear stiffness matrix is calculated by employing this mode shape. Subsequently, the set of nonlinear problem is solved to gain the nonlinear frequency as well as a new corresponding mode shape preliminarily. The later nonlinear stiffness corresponding to this recent mode shape is then computed and a revisited nonlinear frequency is thus attained. To fulfill the satisfactory accuracy, this procedure is reiterated until the tolerance is accepted for the frequencies and their corresponding mode shapes. Up to two or three iterations are sufficient in the case of small till moderate amplitudes of vibrations, four to five iterations are ample for the large amplitudes of vibrations.

4. Results and discussions

Both the linear dynamic computational model and the nonlinear dynamic counterpart are verified with other investigations. Brief parameters employed in the calculations are taken down in Table 1.

Table 2 exhibits the comparisons of the linear fundamental frequencies for an almost upright riser/pipe with hinge ends among each model, under various internal flow velocities. Apparently, the results obtained are in very good agreement. The lateral modes

Table 1
General material properties of marine risers/pipes

Emblematic list		Value	Unit
Top tension	T_H	476.198	kN
Sea depth	H	300	m
Static offset	X_H	0	m
Riser's weight in air	W	7850	kg/m
Outer diameter	D_O	0.26	m
Riser's thickness	t	0.03	m
Sea density	ρ_w	1025	kg/m
Internal fluid density	ρ_I	998	kg/m
Modulus of elasticity	E	2.07×10^8	kN/m^2
Inertia coefficient	C_m	2	
Normal drag force coefficient	C_{Dn}	0.7	
Tangential drag force coefficient	C_{Dt}	0.03	
Current velocities	V_c	0	m/s

(w-mode) expose the dominance over longitudinal modes (u-mode) for which corresponding to their frequencies.

As aforementioned, the nonlinear free vibrations of marine risers/pipes transporting fluid are unexampled. Consequently, the nonlinear dynamic model is validated via the application of the identical formulations to nonlinear beams. The adjustment is executed by re-imposing the support conditions to be at the same level and by depriving the internal fluid. Table 3 takes the role of the nonlinear fundamental frequencies for an upright pipe or a straight beam, as illustrated by Fig. 2. The nonlinear frequency ratios $[\omega_N/\omega_L]^2$ are manifested versus the non-dimensional amplitudes of vibration a/r, where r is the radius of gyration. It is found that nonlinear hinged beams give the hardening phenomenon, a vibrating behavior that the frequencies increase up to the amplitudes of vibration do. The Fig. 2 delineates a good agreement of the nonlinear results with those reported by others

Table 2
Comparison of linear fundamental frequencies

Internal flow velocity (m/s)	References		This study	%Difference from analytic solution[a]
	Analytic solution[a]	GFEM[b]		
0	0.2878	0.2891	0.2890	0.4170
5		0.2881	0.2881	
10	0.2838	0.2853	0.2852	0.4933
15		0.2804	0.2803	
20	0.2706	0.2731	0.2730	0.8869
25		0.2627	0.2627	
30	0.2413	0.2478	0.2478	2.6937
35		0.2224	0.2221	
37		–	0.1962	
38		0.1710	Unstable	
39		Unstable		

[a] Moe and Chucheepsakul, 1988.
[b] Chucheepsakul et al., 1999.

Table 3
Nonlinear fundamental frequencies of the calibrated beam

a/r	Nonlinear fundamental frequency ratio $(\omega_N/\omega_L)^2$				
	Exact[a]	GFEM[b]	RQFEM[c]	FEM[d]	This study ($L/r=971$)
0.00	1.0000	1.0000	1.0000	1.0000	1.0000
0.10	1.0025	1.0025	1.0025	1.0018	1.0023
0.20	1.0100	1.0100	1.0100	1.0074	1.0092
0.40	1.0400	1.0400	1.0400	1.0298	1.0369
0.60	1.0900	1.0900	1.0900	1.0689	1.0831
1.00	1.2500	1.2499	1.2500	1.1857	1.2311
1.50	1.5625	1.5624	1.5625	1.4166	1.5205
2.00	2.0000	1.9998	2.0000	1.7379	1.9265
2.50	2.5625	–	2.5625	–	2.4499
3.00	3.2500	3.2495	3.2500	2.6439	3.0923

Note that: GFEM, Galerkin Finite Element Method; RQFEM, Rayleigh Quotient Finite Element Method; FEM, Finite Element Method.

[a] Woinowsky-Krieger, 1950.
[b] Bhashyam and Prathap, 1980
[c] Sarma and Varadan, 1983.
[d] Mei, 1973.

(Mei, 1973; Moe and Chucheepsakul, 1988; Paidoussis, 1998; Patel and Witz, 1991), however, it is noted that the slenderness ratio $L/r=971$ is utilized in this reckoning. Thus, the model developed is valid to scrutinize the nonlinear vibrating characteristics of marine risers/pipes as above-mentioned.

Prior to studying the nonlinear dynamic analyses, the parameters involved in the investigations are introduced by the clustering of the dispersed variables as follows.

Parameter Δ

An expedience in general (Patel and Witz, 1991; Lin and Tsai, 1997), this dimensionless parameter is taken parts in by a variety of variables: the moment of inertia

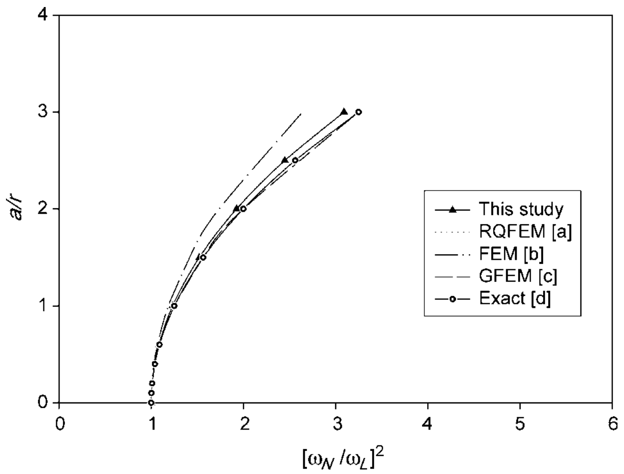

Fig. 2. Nonlinear frequency ratios $[\omega_N/\omega_L]^2$ of the calibrated beam.

I, the modulus of elasticity E, the top tension T_H, and the riser/pipe's length L. The parameter is given by

$$\varDelta = \frac{EI}{T_{\mathrm{H}} L^2} \tag{49}$$

Parameter μ

Facilitating the study on the effects of internal flow, the internal flow parameter unites the internal flow velocity V, the internal fluid density ρ_i, the riser's internal cross-section A_i, and the top tension into a simpler form of

$$\mu = V \sqrt{\frac{\rho_i A_i}{T_{\mathrm{H}} - \rho_i A_i V^2}} \tag{50}$$

Parameter Λ

On the role of static offsets in nonlinear characteristics, the third parameter referred to as an offset percentage contains the static offset X_H and sea depth H. Its expression is arranged to

$$\Lambda = \frac{X_H}{H} \tag{51}$$

4.1. Parametric effect of $\varDelta$

A nearly vertical riser is perused with various moduli of elasticity and top tensions to sketch the unprecedented nonlinear dynamic characteristics of the marine riser/pipe transporting fluid. The basic data used in the computation follows the Table 1. Exceptionally, the moduli of elasticity E are varied between 2.07×10^7 and 2.07×10^{10} kN/m^2 and the top tensions T_H are calculated from 450 to 1000 kN. Involving the top tensions T_H and flexural rigidity EI, two cases are discussed herein: first, effect of a variation in T_H while EI is fixed; and later, effect of a variation in EI while another is fixed.

Case I: Role of top tensions

Fig. 3 portrays the nonlinear fundamental frequencies of the riser relative to the linear counterpart. Meaning the high rise of top tensions, the small amount of $\varDelta$ has a considerable influence on the nonlinear frequencies. At moderate to high top tensions, for all conditions, the nonlinear vibrational behavior is categorized into hardening type, a dynamic characteristic the frequency increases in amplitude of vibration. This occurrence is attributed to the top tension, substantially mounting the stretching stiffness. While the amount of $\varDelta$ rising, the nonlinear behavior gradually becomes softening type, a dynamic quintessence the frequency diminishes in thriving amplitude of vibration. The softening characteristic found is in accordance with that in other structures under compression like the arch problems.

Case II: Role of the flexural rigidity

The variation of the nonlinear frequency ratio $(\omega_N/\omega_L)^2$, influenced by the flexural rigidity, is depicted in Fig. 4. Obviously the flexural rigidity EI plays significant role in

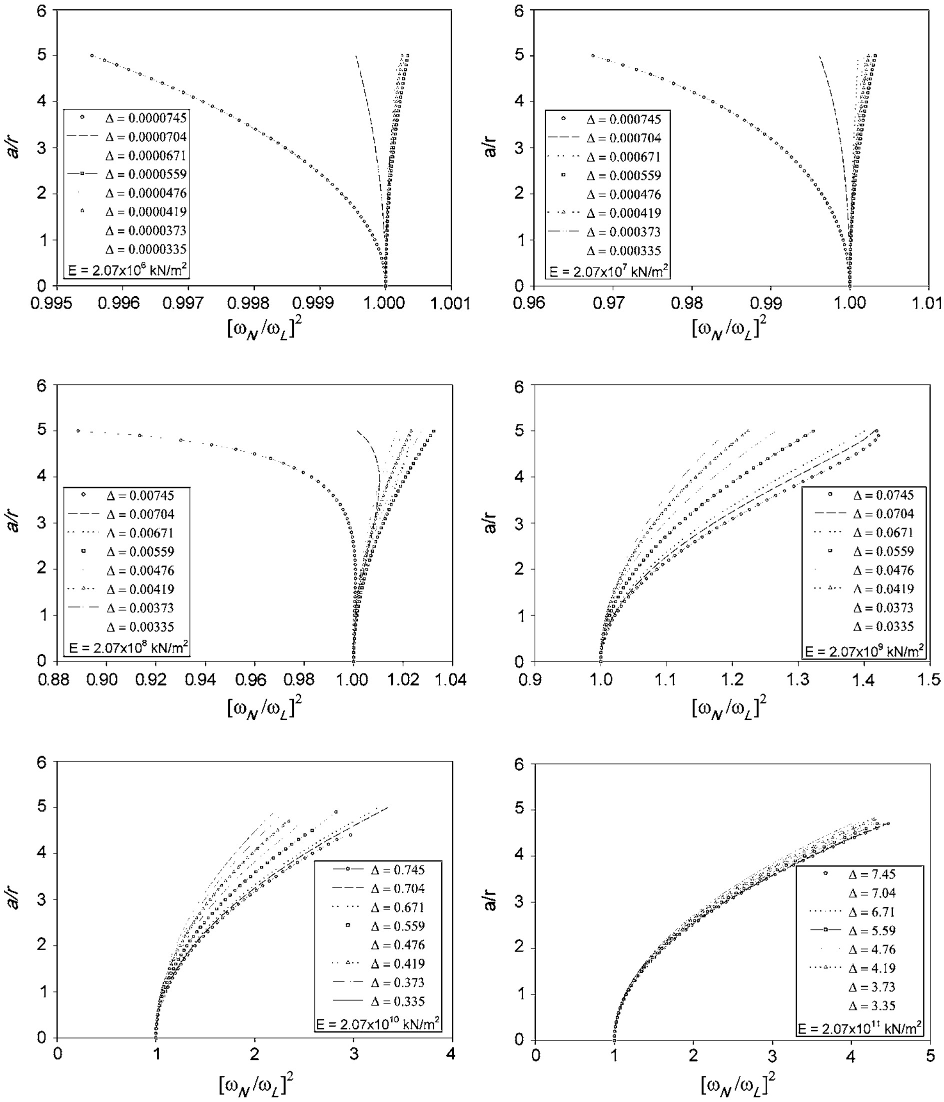

Fig. 3. Parametric effect of Δ in the relation between nonlinear frequency ratios $[\omega_N/\omega_L]^2$ and amplitude of vibration (a/r): role of top tensions.

the nonlinear frequency domain. The small figures of Δ, representing the low flexural rigidity, subtly indicate the nonlinear frequency ratios as the softening type. However, the higher ranges demonstrate the hardening dynamic characteristic of the riser/pipe similar to those in such flexural members as the beams, girders, plates, etc. Graphically, it is found that the flexural rigidity affects the dynamic behaviors of marine risers/pipes more meaningfully than the top tensions do.

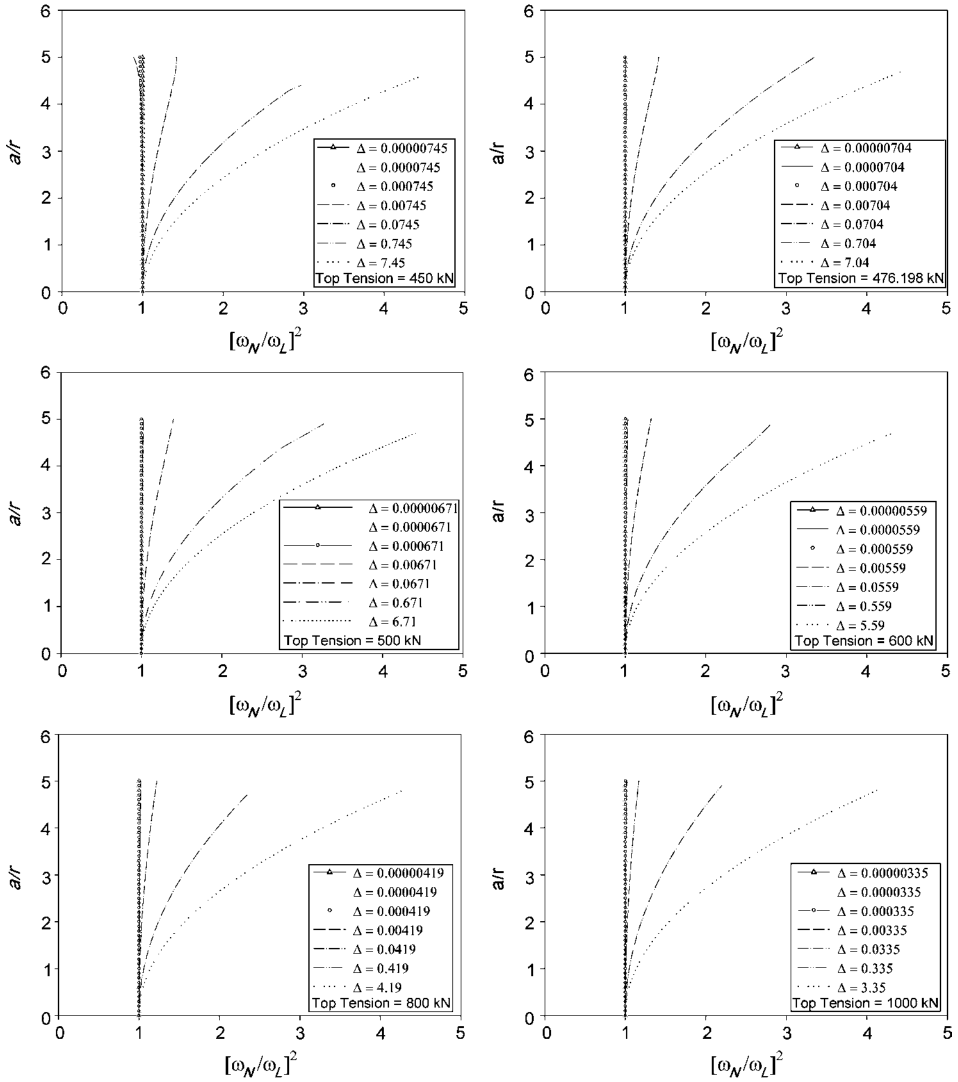

Fig. 4. Parametric effect of Δ in the relation between nonlinear frequency ratios $[\omega_N/\omega_L]^2$ and amplitude of vibration (a/r): role of the flexural rigidity.

Fig. 5 displays the dominant, nonlinear, fundamental mode shapes (u-mode) of the marine risers/pipes for the calibrated case: the modulus of elastic $E = 2.07 \times 10^8$ kN/m^2. Dependently on the magnitude of top tensions, the dynamic mode shapes as well as their reversal points always shift downward while the amplitude of vibration increases. The lower top tension allows much gravitational downward movement more than the upper range consents due to the stretching occurrence along the riser/pipe. The downward movement compulsorily causes the softening type of dynamic behavior. Reasonably, it is

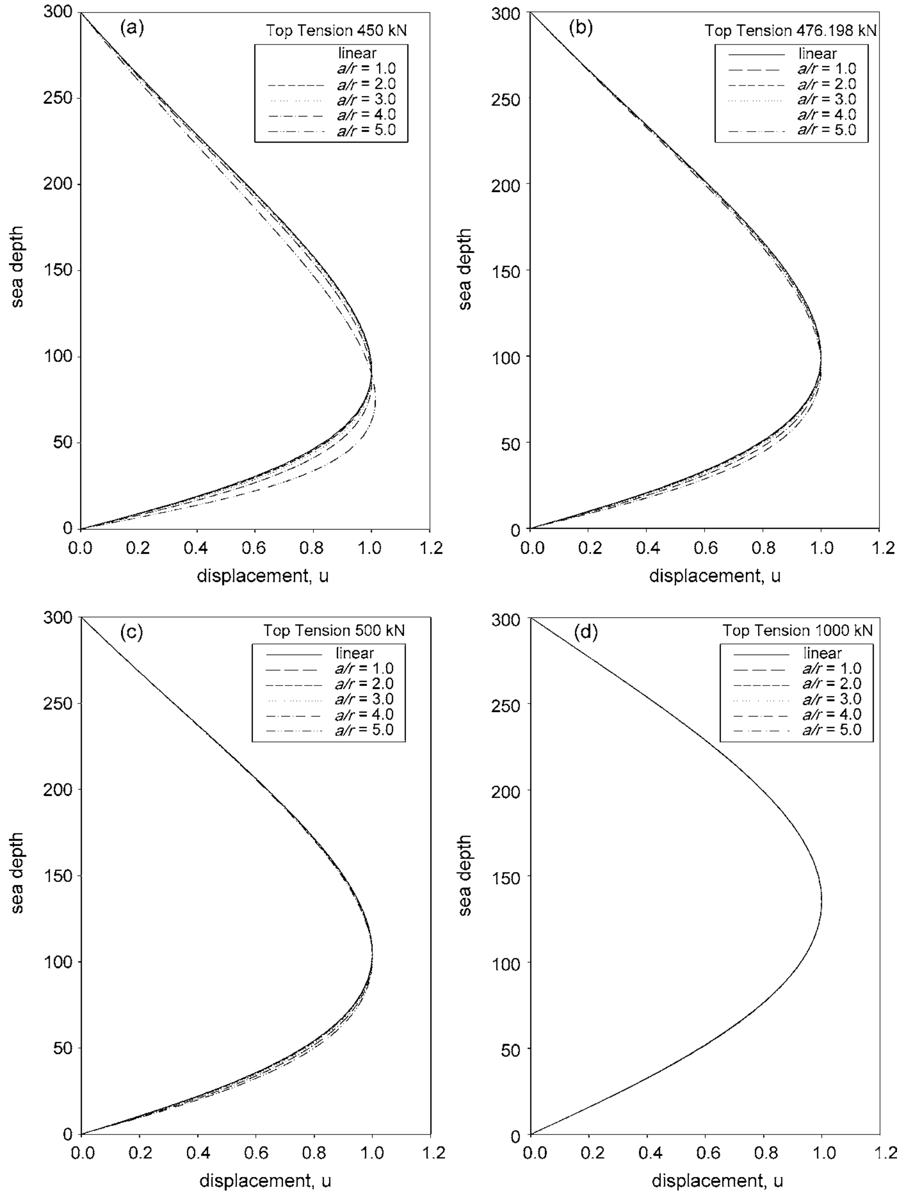

Fig. 5. Nonlinear mode transfigurations of marine risers/pipes under the parametric effect of Δ.

noticeable that the reversal point is lower than the middle point of sea depth. The displacement fields, employed in the nonlinear stiffness, decrease in the part above the reversal point much more than increase in the bottom part. Thereby the nonlinear stiffness is slightly diminished, and then, the softening characteristic appears by degrees. Differently, at moderate to high top tensions, the displacement fields have both upper and lower parts increase, although they are small in the upper part. They evidently form the increasing nonlinear stiffness and then the hardening characteristic manifests. At the very high top tensions, it is found that the mode configuration is almost unchanged due to the rigorous stretching force. The lesser displacement fields provide the smaller increasing nonlinear stiffness and the lower degree of hardening in the dynamic behavior of the riser/pipe. As a beam-column-like structure or a flexural-compression member with varied tension, the riser/pipe exhibits both nonlinear dynamic characteristics simultaneously: softening and hardening types depending on its rigidity, axial burdens, and amplitude of vibration.

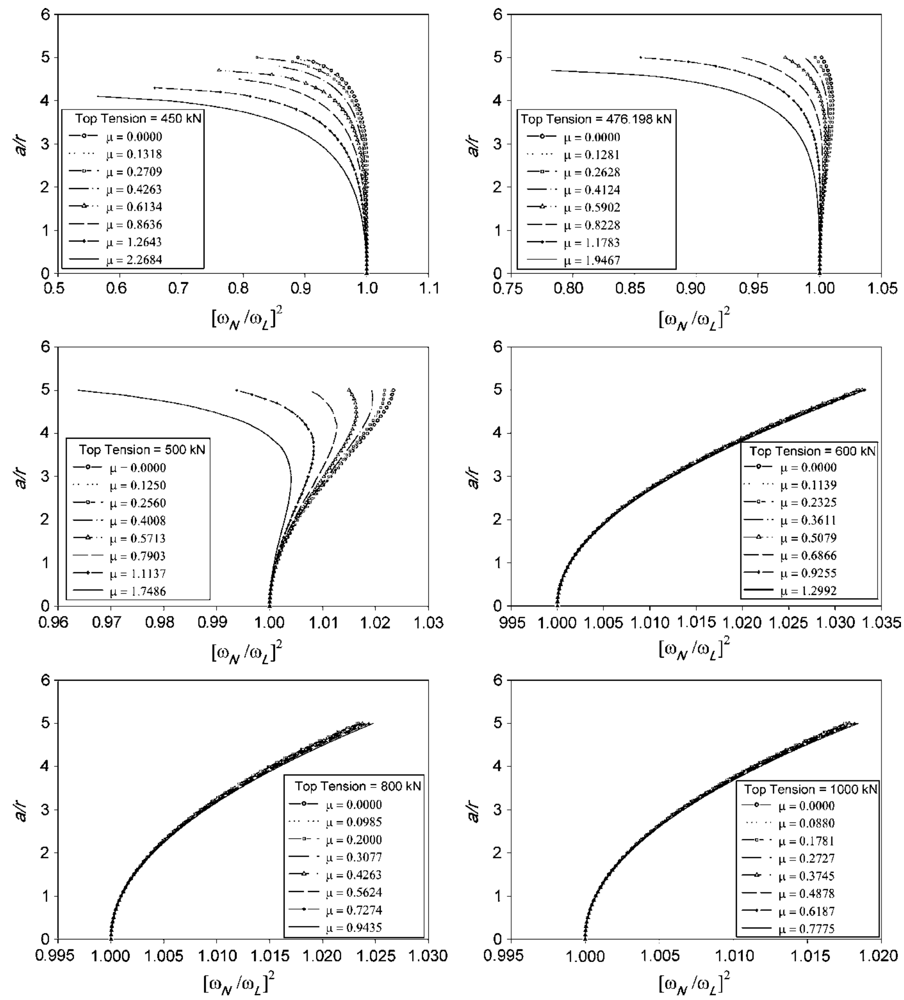

Fig. 6. Parametric effect of μ in the relation between nonlinear frequency ratios $[\omega_N/\omega_L]^2$ and amplitude of vibration (a/r).

4.2. Parametric effect of μ

In order to ascertain the nonlinear behavior due to the parameter μ, the riser's properties used in the parametric study are in the Table 1. The variation of internal flow velocity is

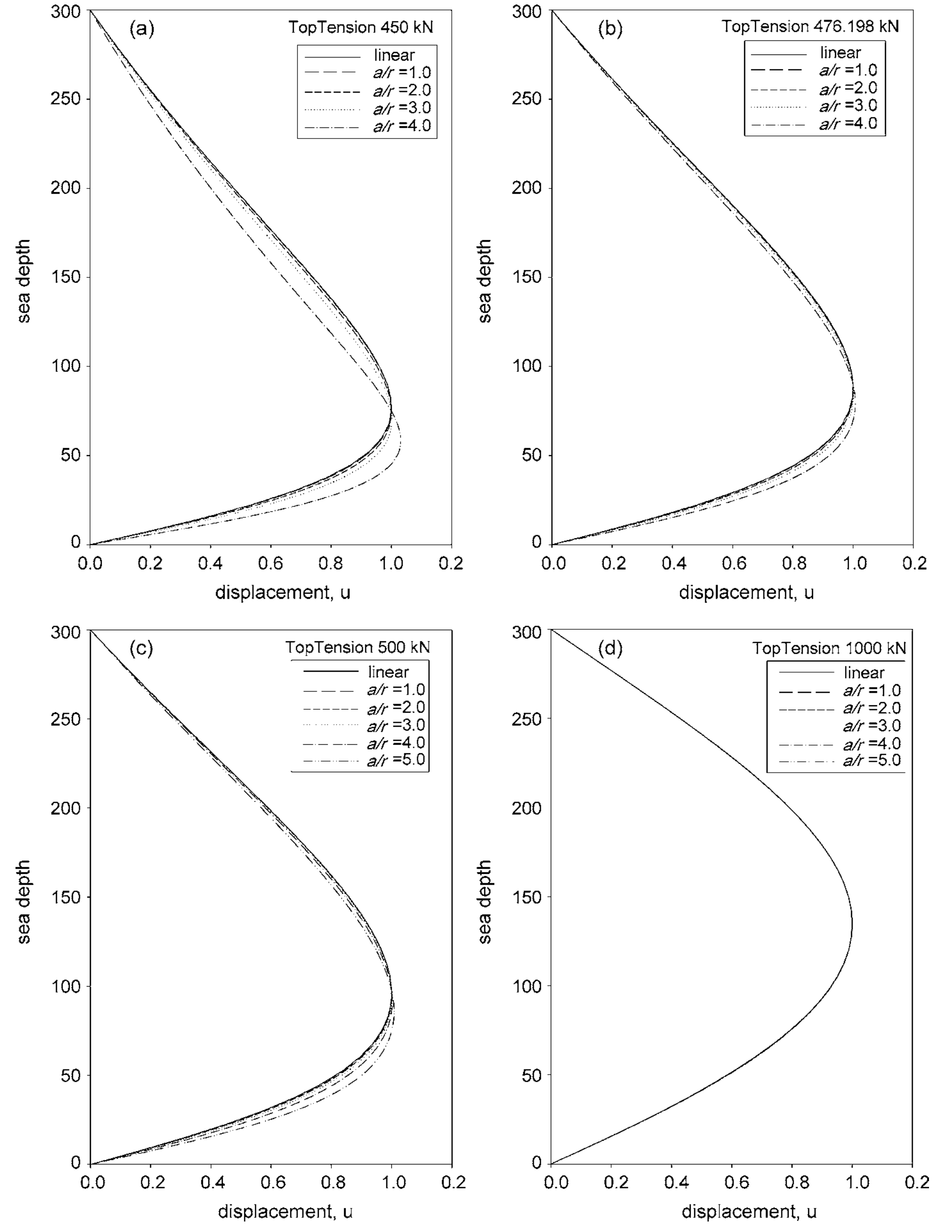

Fig. 7. Nonlinear mode transfigurations of marine risers/pipes under the parametric effect of μ.

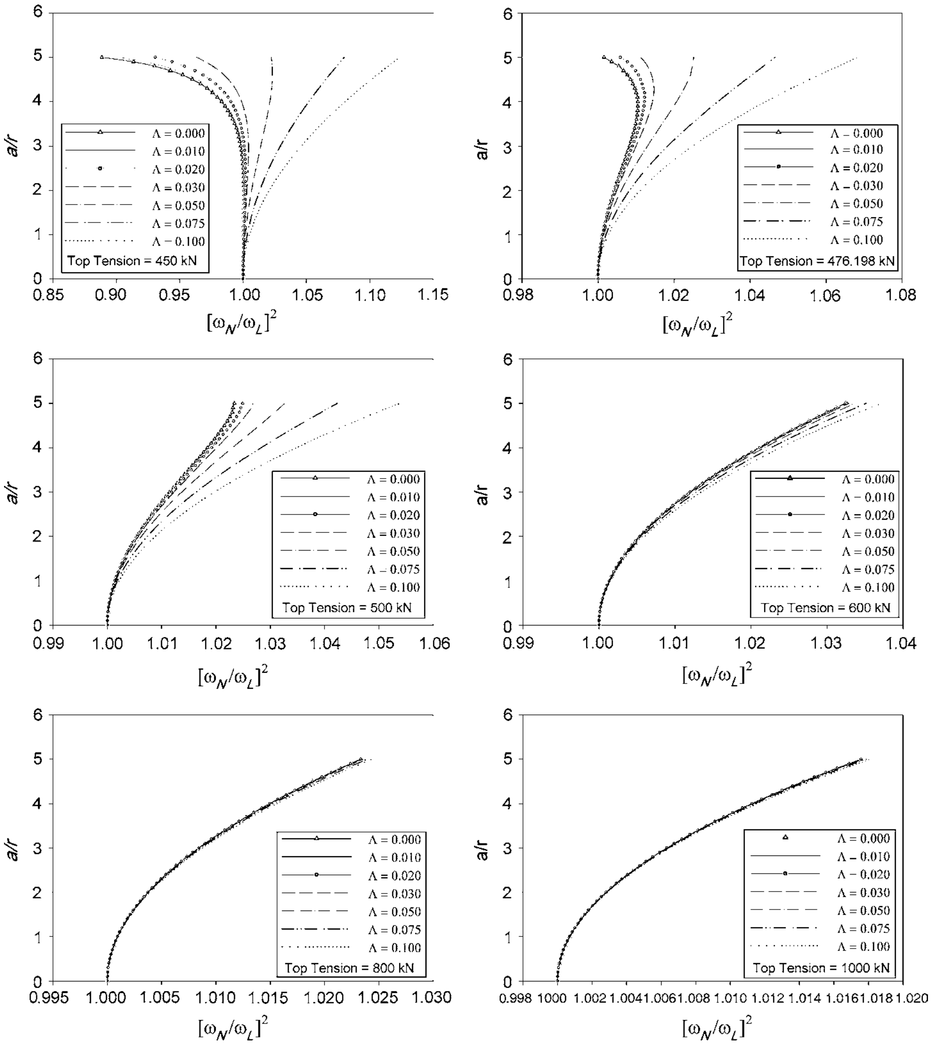

Fig. 8. Parametric effect of Λ in the relation between nonlinear frequency ratios $[\omega_N/\omega_L]^2$ and amplitude of vibration (a/r).

between 0 and 35 m/s. Fig. 6 marks the influence of internal flow on the nonlinear fundamental frequency ratios of the marine risers/pipes. The internal flows exponentially reduce the top tension values thus they tend to decrease the degree of hardening and increase the degree of softening in the nonlinear dynamic phenomenon at the low to moderate top tensions. In higher values of top tension, it is found that the internal flow velocities have less participation in the nonlinear features since their amounts are deficient to weaken the very high values of top tensions.

The prominent corresponding dynamic mode shapes (u-mode) are illustrated in Fig. 7. Not only does the internal flow speed diminish the top tensions but clearly it also lowers

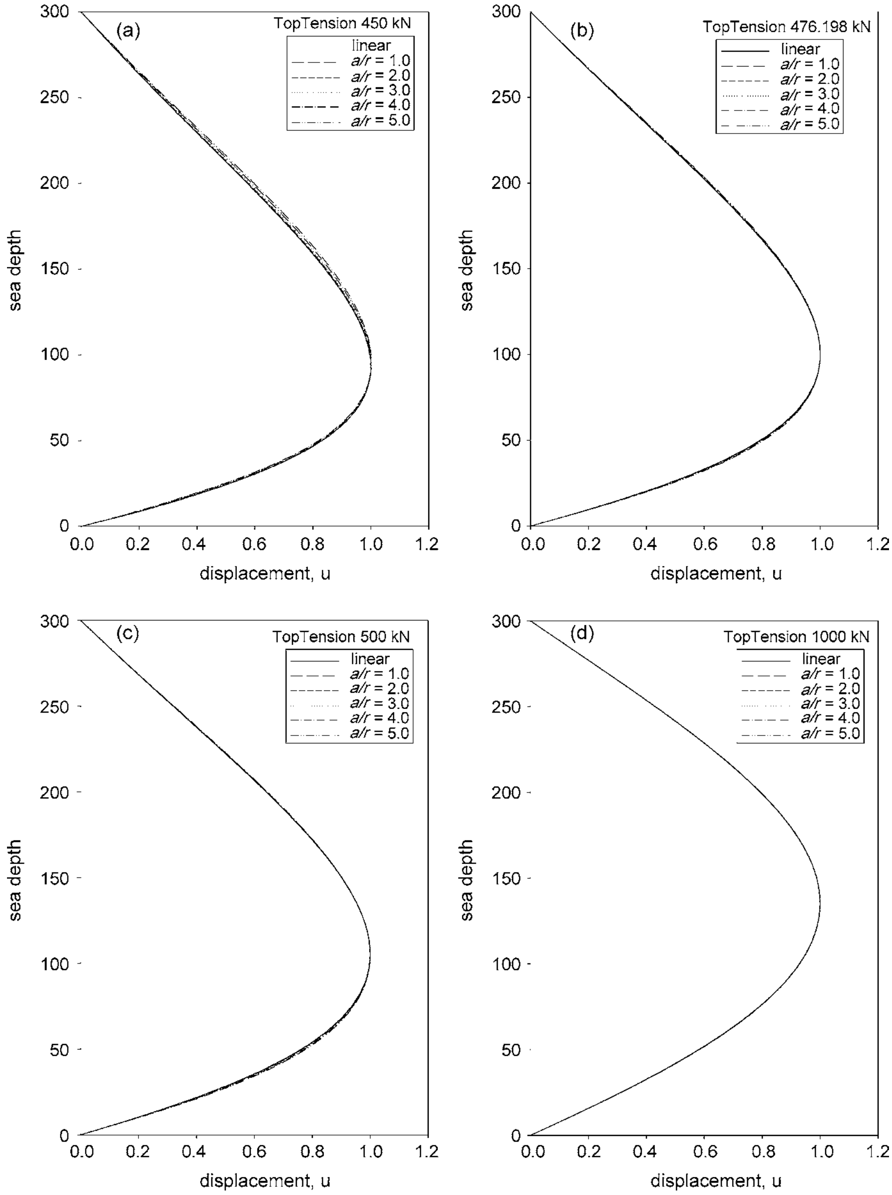

Fig. 9. Nonlinear mode transfigurations of marine risers/pipes under the parametric effect of Λ.

the reversal point of the mode configuration. As a result, the nonlinear stiffness, decreased by the swift displacement-field shrinkage, tends to specify the nonlinear dynamic characteristics. As witnessed previously, the nonlinear dynamic phenomenon relies on the effective tension range conceived along the riser/pipe length. The hardening type exists when the effective tension is beyond a medium figure and the softening type dawns when the value descends beneath the criterion.

4.3. Parametric effect of Λ

The parameter Λ reveals the role of static offsets on the nonlinear dynamic behavior of the risers/pipes. Utilized in the calculation, the material properties are shown in Table 1. Additionally, the horizontal static offsets, confronting the current and wave forces, are in the various spacing ranges from 0 to 30 m. (0–10% Offset) The nonlinear frequency ratios, ascribed to a variation of the top offsets, are described in Fig. 8. Spectacularly, the static offsets have a momentous influence on the riser dynamics. In the softening characteristic, they reduce the degree of softening and also stiffen the degree of hardening in the dynamic characteristic of hardening type. The offsets play more crucial role in the dynamic characteristic at the low to moderate top tensions than at the higher values of the top tensions.

Mode transfigurations due to the parametric effect are graphically shown in Fig. 9. Distinctly, the static offsets influence the distinguished increments in the upper part of mode shapes and the bit increments in the lower part. Owing to the nonlinear stiffness become larger, the hardening characteristic subsequently prevails over the softening type. The transformation of the mode shapes tends to raise the reversal point, and then, its indication predominates the dynamic characteristic of the structure.

5. Conclusions

The investigation on nonlinear free vibrations of marine risers/pipes transporting fluid is presented in this paper. The finite element model is verified with existing results in literature and they are found in good agreement. Obtained from the modified direct iteration incorporating with the inverse iteration, the numerical results are illustrated to demonstrate the parametric effects.

The dynamic characteristics of the parametric studies indicate that the flexural rigidity has a remarkable influence on the nonlinear traits by stiffening the degree of vibrations: softening to hardening, and hardening to higher degree. Top tensions are in the significant point of view in stretching the nonlinear mode shapes. Exponentially weakening the axial stretching, the internal flows clearly reduce the degree of hardening and tend to turn the vibration type from hardening to softening one. At all cases, the static offsets conspicuously stiffen the degree of vibration since they perturb the top end and then contribute to the farther locomotion at the upper part. The key indication of nonlinear dynamic traits is the shift of mode shapes. The softening characteristic tends to arise when the mode shapes shift downward, and on the other hand, the hardening type tends to be born when the mode shapes move upward.

Acknowledgements

This research is sponsored by the Thailand Research Fund under grant RTA/03/2543. The authors are grateful to acknowledge the financial support.

References

Atadan, A.S., Calisal, S.M., Modi, V.J., Guo, Y., 1997. Analytical and numerical analysis of the dynamics of a marine riser connected to a floating platform. Ocean Engineering 24 (2), 111–131.

Bar-Avi, P., 2000. Dynamic response of risers conveying fluid. Journal of Offshore Mechanics and Arctic Engineering 122, 188–193.

Bhashyam, G.R., Prathap, G., 1980. Galerkin finite element method for nonlinear beam vibrations. Journal of Sound and Vibration 72 (2), 191–203.

Chucheepsakul, S., Huang, T., 1994. Influence of transported mass on the equilibrium configuration of risers, Proceedings of the Fourth International Offshore and Polar Engineering Conference. Osaka, Japan, vol. 2 1994 pp. 246–249.

Chucheepsakul, S., Huang, T., Monprapussorn, T., 1999. Influence of transported fluid on behavior of an extensible flexible riser/pipe, Proceedings of the Ninth International Offshore and Polar Engineering Conference. Brest, France, vol. 2 1999 pp. 286–293.

Chucheepsakul, S., Huang, T., Monprapussorn, T., 2001. Stability analysis of extensible flexible marine pipes transporting fluid, Proceedings of the 11th International Offshore and Polar Engineering Conference. Stavanger, Norway, vol. 2 2001 pp. 722–729.

Chucheepsakul, S., Monprapussorn, T., Huang, T., 2003. Large strain formulations of extensible flexible marine pipes transporting fluid. Journal of Fluids and Structures 17 (2), 185–204.

Chung, J.S., Cheng, B.R., Huttelmaier, H.P., 1994a. Three-dimensional coupled responses of a vertical deep-ocean pipe: part I. Excitation at pipe ends and external torsion. International Journal of Offshore and Polar Engineering 4 (4), 320–330.

Chung, J.S., Cheng, B.R., Huttelmaier, H.P., 1994b. Three-dimensional coupled responses of a vertical deep-ocean pipe: part II. Excitation at pipe top and external torsion. International Journal of Offshore and Polar Engineering 4 (4), 331–339.

Cook, R.D., Malkus, D.S., Plesha, M.E., 2002. Concepts and Applications of Finite Element Analysis, fourth ed. Wiley, New York.

Furnes, G.K., 2000. On marine riser responses in time- and depth-dependent flows. Journal of Fluids and Structures 14, 257–273.

Huang, T., 1993. Kinematics of transported mass inside risers and pipes, Proceedings of the Third International Offshore and Polar Engineering Conference, Singapore, vol. 2 1993 pp. 331–336.

Huang, T., Chucheepsakul, S., 1985. Large displacement analysis of a marine riser. Journal of Energy Resources Technology 107 (2), 54–59.

Huang, T., Kang, Q.L., 1991. Three dimensional analysis of a marine riser with large displacements. International Journal of Offshore and Polar Engineering 1 (4), 300–306.

Irani, M.B., Modi, V.J., Welt, F., 1987. Riser dynamics with internal flow and nutation damping, Proceedings of the Sixth International Offshore Mechanics and Arctic Engineering Conference. Houston, USA, vol. 3 1987. 119–125.

Kaewunruen, S., 2003. Nonlinear free vibrations of marine risers/pipes transporting fluid. Master of Engineering Thesis. Department of Civil Engineering, KMUTT. 156p.

Lin, Y.H., Tsai, Y.K., 1997. Nonlinear vibrations of Timoshenko pipes conveying fluid. International Journal of Solids and Structures 34, 2945–2956.

Mei, C., 1973. Finite element displacement method for large amplitude free vibrations of beams and plates. Computers and Structures 3, 163–174.

Moe, G., Chucheepsakul, S., 1988. The effect of internal flow on marine risers, Proceedings of the Seventh International Offshore Mechanics and Arctic Engineering Conference, Houston, USA, vol. 1 1988 pp. 375–382.

Païdoussis, M.P., 1998. Fluid-Structure Interactions: Slender Structures and Axial Flow, vol. 1. Academic Press, London.

Patel, M.H., Witz, J.A., 1991. Compliant Offshore Structures. CRC Press, New York.

Sarma, B.S., Varadan, T.K., 1983. Lagrange-type formulation for finite element analysis of nonlinear beam vibrations. Journal of Sound and Vibration 86 (1), 61–70.

Tikhonov, V.S., Safronov, A., Kamyshev, M.A., Figarov, N.G., 1996. Numerical analysis of pipeline dynamics in seabed laying. International Journal of Offshore and Polar Engineering 6 (3), 212–218.

Woinowsky-Krieger, S., 1950. The effect of an axial force on the vibration of hinged bars. Journal of Applied Mechanics 17, 35–36.

Wu, M.C., Lou, J.Y.K., 1991. Effects of rigidity and internal flow on marine riser dynamics. Applied Ocean Research 13 (5), 235–244.